coatings

MDPI

Article

Microwave-Assisted Dip Coating of *Aloe Vera* on Metallocene Polyethylene Incorporated with Nano-Rods of Hydroxyapaptite for Bone Tissue Engineering

Hairong Wang [1], Xueliang Zhang [2], Mohan Prasath Mani [3], Saravana Kumar Jaganathan [4,5,6,*], Yi Huang [1] and Chengzheng Wang [1]

1 Department of Orthopedics, Jianhu Hospital Affiliated to Nantong University, Yancheng 224700, China; whr325@163.com (H.W.); hy20465@163.com (Y.H.); wangcz1983@163.com (C.W.)
2 Department of Orthopedics, First Hospital of Lanzhou University, Lanzhou 730000, China; z540382252@163.com
3 Faculty of Biosciences and Medical Engineering, Universiti Teknologi Malaysia, Johor Bahru 81300, Malaysia; mohanprasathutm@gmail.com
4 Department for Management of Science and Technology Development, Ton Duc Thang University, Ho Chi Minh City, Vietnam
5 Faculty of Applied Sciences, Ton Duc Thang University, Ho Chi Minh City, Vietnam
6 IJN-UTM Cardiovascular Engineering Centre, Department of Clinical Sciences, Faculty of Biosciences and Medical Engineering, Universiti Teknologi Malaysia, Johor Bahru 81300, Malaysia
* Correspondence: saravana@tdt.edu.vn

Academic Editor: Mazeyar Parvinzadeh Gashti
Received: 18 August 2017; Accepted: 14 October 2017; Published: 31 October 2017

Abstract: Bone tissue engineering widely explores the use of ceramic reinforced polymer-matrix composites. Among the various widely-used ceramic reinforcements, hydroxyapatite is an undisputed choice due to its inherent osteoconductive nature. In this study, a novel nanocomposite comprising metallocene polyethylene (mPE) incorporated with nano-hydroxyapaptite nanorods (mPE-nHA) was synthesized and dip coated with *Aloe vera* after subjecting it to microwave treatment. The samples were characterized using contact angle, Fourier transform infrared spectroscopy (FTIR), scanning electron microscope (SEM), atomic force microscopy (AFM) and 3D Hirox microscopy scanning. Contact angle results show that the hydrophilicity of mPE-nHA improved notably with the coating of *Aloe vera*. The surface topology and increase in surface roughness were observed using the SEM, AFM and 3D Hirox microscopy. Blood compatibility assays of pure mPE and the *Aloe vera* coated nanocomposite were performed. The prothrombin time (PT) was delayed by 1.06% for 24 h *Aloe-vera*-treated mPE-nHA compared to the pristine mPE-nHA. Similarly, the 24 h *Aloe-vera*-coated mPE-nHA nanocomposite prolonged the activated partial thromboplastin time (APTT) by 41 s against the control of pristine mPE-nHA. The hemolysis percentage was also found to be the least for the 24 h *Aloe-vera*-treated mPE-nHA which was only 0.2449% compared to the pristine mPE-nHA, which was 2.188%. To conclude, this novel hydroxyapatite-reinforced, *Aloe-vera*-coated mPE with a better mechanical and anti-thrombogenic nature may hold a great potential to be exploited for bone tissue engineering applications.

Keywords: metallocene polyethylene; hydroxyapatite nanorods; *Aloe vera* coating; bone tissue engineering

1. Introduction

In biomedical applications, the materials used for bone tissue engineering must possess certain characteristics, such as being biocompatible, biodegradable, non-toxic, highly porous, have significant mechanical properties and should not cause foreign body reactions [1]. Recently, many researchers utilized the variety of materials in repairing the damaged tissue. The utilized materials were polymers, metals, and ceramics. The use of metals and ceramics in bone tissue engineering were limited owing to certain limitations such as a lack of degradability in a biological environment and limited process ability [2]. Alternatively, today these polymers are widely used in bone tissue engineering owing to their design flexibility and the fact that they can be easily tailored according to specific needs [3]. The frequently used polymers for making nanocomposites in bone tissue engineering are poly (lactic acid), poly (glycolic acid), poly (lactic-co-glycolic acid), poly (caprolactone) and natural polymers such as collagen, gelatin, silk, and chitosan. Several nanoparticle-reinforced polymer composites have been fabricated for bone tissue engineering applications. It was found that a 10% nano-particle reinforcement, by weight, enhances the stiffness and strength of the polymeric matrix, yet decreases the toughness [4]. On the other hand, a >10% increase of nHA reduces the mechanical properties due to a marked clustering effect of nano-particles [5]. The chemical formula of HA is $Ca_{10}(PO_4)_6(OH)_2$ and it is known as pentacalcium hydroxide tris (orthophosphate) [6–8]. In the last twenty years, enormous attention has been given to the HA-based filler reinforcement for polymer matrices for plausible biomedical applications such as tissue engineering [9]. Hence, there is increasing interest in the development of novel hybrids and nano-powders to be incorporated into suitable polymers to confer better mechanical properties [10–12].

Aloe vera is a commonly available plant that has been increasingly used in the day-to-day life of human beings. The succulent part of the plant contains numerous potentially active substances in the form of essential amino acids, glucomannans, minerals, lipids, vitamins, polysaccharides, major polypeptides, proteins, and antioxidants [13,14]. In the mid-1990s the total sales value of products composed of *Aloe vera* derivatives and ingredients was reported to be $1 billion; since then it has grown tremendously and now it is estimated to be more than $35 billion globally [15]. Meanwhile, exhaustive research has been conducted to scrutinize the therapeutic propensity of *Aloe vera*. These studies have revealed its ability to promote tissue regeneration or rehabilitation by improving oxygen and blood supply, shielding from microbial attacks, and providing essential nourishment [16]. Hence, in this work, *Aloe vera* extract is utilized to develop an antifouling and biocompatible biomaterial for bone implant applications.

Microwaves are radio waves possessing wavelengths from one millimeter to one meter, or equivalent, with frequencies between 300 MHz (0.3 GHz) and 300 GHz. In recent times, microwaves have been used successfully for the surface modification of polymers and fabrics [17,18]. The cost, time, and energy requirements of microwave treatment are significantly lower compared to other surface treatment methods. Besides that, the size of the microwave system is compact in comparison to other techniques because of the high energy applicators and direct energy absorption by most of the materials. In addition, good instantaneous control and decreased environment pollution are some of the chief benefits which promote microwave treatment as a better tool for surface modification [19].

Apart from the selection of the most suitable filler, there are other critical factors, such as the effective dispersion and distribution of filler into the matrix by the prevention of agglomeration [20], introducing H-bonds [21], or the functionalization of the filler. These are the pre-requisite vital factors to enhancing the affinity between the filler and polymer, to create surface roughness, to tailor the aspect ratio of filler (2D) and to increase interfacial adhesion in polymer nanocomposites [22,23]. Until now, a complete understanding of the correlation between all these factors is a daunting challenging for novel biomedical applications. An extensive literature review has revealed numerous studies that report the synthesis of hydroxyapatite in various forms and shapes, such as spherical, rod-like, fiber-like and flower-like [24–26] via different methods such as hydrothermal, microwave and precipitation methods. Nevertheless, there are no available reports on the preparation of hydroxyapatite nanorods with a high

aspect ratio embedded with mPE to form rod-like HA/mPE nanocomposites. The present investigation aims to develop a microwave-assisted *Aloe vera* coating on the novel mPE-nHA nanocomposite for bone tissue engineering applications.

2. Materials and Methods

2.1. Blood Procurement and Ethical Approval

All the experimental procedures involved in the handling of blood were approved by the Faculty of Biosciences and Medical Engineering, Universiti Teknologi Malaysia with ref no: UTM.J.45.01/25.10/3Jld.2(3). A group of healthy adults was recruited and educated regarding the risks and benefits of blood donation. The participants were given sufficient time to decide whether they would like to participate in the study or not. The blood was withdrawn via venipuncture after getting the signature on the consent form. Then, the freshly-drawn whole blood was anticoagulated with acid-citrate-dextrose (56 mM sodium citrate, 65 mM citric acid, 104 mM dextrose, CCD) at a ratio of 9:1 (blood/citrate). Finally, the platelet poor plasma (PPP) was obtained by centrifuging the citrated blood at 3000 rpm for 15 min using Heraeus Labofuge™ 200 centrifuge (Thermo Fischer Scientific, Waltham, MA, USA).

2.2. Chemicals

Calcium nitrate tetrahydrate ($Ca(NO_3)_2 \cdot 4H_2O$) and diammonium hydrogen phosphate (DAHP) ($(NH_4)_2HPO_4$), oligomeric surfactant, polypropylene glycol (PPG M_n ~425), were supplied by Sigma-Aldrich, St. Louis, MO, USA. Aliphatic polyethylene carbonate diol (PCD) (M_w = 1000), with a characteristic OH value of 57.0 mg KOH/g was used. 4,4′-Methylene bis(phenyl isocyanate) (MDI) and 1,4-butanediol (BD) were obtained from Sigma-Aldrich, St. Louis, MO, USA. Solvents such as Tetrahydrofuran (THF), acetone and methanol were of analytical grades and were supplied by Merck, Darmstadt, Germany.

2.3. Synthesis of Hydroxyapatite Nanorods

Hydroxyapatite nanorods of higher aspect ratios was prepared by using non-ionic surfactant e.g., polypropylene glycol in normal atmospheric condition for the first time. In a beaker, 0.2 $mol \cdot L^{-1}$ each of $Ca(NO_3)_2 \cdot 4H_2O$ and $(NH_4)_2HPO_4$ in 500 mL of double distilled water were taken in amounts such that Ca:P mole ratio was maintained at ~1.67. We followed an in-situ technique for the preparation of PPG-coated nHA rods; 5 wt % (with respect to Calcium and Phosphate precursors) of PPG was added to the solution of calcium nitrate as a non-ionic surfactant as well as the coating agent to improve the interfacial adhesion between the thermoplastic polyurethane (TPU) and nHA while preparing nanocomposites. The pH of both the calcium nitrate and DAHP solutions were maintained at ~11 to 12 with the addition of the required amount of NH_4OH solution. Then $(NH_4)_2HPO_4$ was added drop-wise to the mixture of $Ca(NO_3)_2 \cdot 4H_2O$ & PPG and the whole milky suspension was vigorously stirred at 70 °C using a mechanical stirrer (2800 rpm). The pH of the reaction mixture was also maintained in the range of 11–12 by adding NH_4OH solution gradually (drop-wise). This process was continued for 4 h at 80 °C. HA particles were washed using ethanol, dried, and ground into fine powders for later use (Selvakumar et al. 2015 [27]). Thus, the pristine (unmodified) and PPG-coated HA nanorods are designated as nHA and PPG-nHA, respectively. The nHA crystals were formed as per the following reaction:

$$10Ca(NO_3)_2 \cdot 4H_2O + 6NH_4H_2PO_4 + 2NH_4OH \rightarrow Ca_{10}(PO_4)_2(OH)_2 + 8NH_4NO_3 + 12HNO_3$$

The white gelatinous precipitate thus obtained was filtered using a centrifugal filtration process (3500 rpm for 10 min), washed a number of times with double-distilled water thoroughly (until neutral) and dried at 90 °C for 15 h and calcined at 400 °C for 6 h. The in-situ modified nHA crystals

(PPG-coated) were not subjected to a calcination process because the oligomeric substances are likely to degrade at 400 °C [27].

2.4. Synthesis of HA Nanorod/mPE Nanocomposites by the In-Situ Technique

In the first step, the calculated amount (1 wt %) of nHA or PPG-nHA was well dispersed in THF and sonicated for 1 h in a 500 mL round-bottom flask in an N_2 atmosphere, followed by the addition of the calculated amount of PCD to the same solution. Later, the whole solution was sonicated for 1 h. MDI and BD were then added to the resultant solution, followed by another round of sonication for 30 min. Ultimately, the reaction was carried out at 60 °C for 6 h, with stirring at a speed of 1000 rpm. Once the reaction was completed, the product was purified by precipitation in cold methanol, followed by repeated washings. The precipitate was then dried in a vacuum oven at 60 °C. The synthesized mPE-nHA films were utilized for further experimentation.

2.5. Aloe Vera Extract Preparation

Fresh succulent leaves of *Aloe vera* were chosen and washed with de-ionized water. The skinny upper part and the yellowish latex part were removed. The semitransparent whitish gel was isolated with a metal ladle. Finally, the gel was mixed thoroughly into a concentrated fibrous extract, which was utilized for the coating of metallocene polyethylene nanohydroxyapeptite (mPE-nHA) samples.

2.6. Microwave Treatment

The samples were subjected to microwave treatment before *Aloe vera* coating as the microwave rapidly accelerates the chemical process, plays a pivotal role in the resulting in a homogeneous coating and even strengthens the coating adhesive [28–32]. Initially, the pristine mPE-nHA sheet was cut into identical square-shaped samples of size 2 cm × 2 cm. These samples were washed with distilled water and 70% ethanol to remove the foreign particles present on the surface. Finally, mPE-nHA samples were exposed to an optimized microwave treatment of 800 W and 2450 MHz produced by a microwave oven (Samsung ME711K, Suwon, Korea) for one minute.

2.7. Dip Coating of Aloe Vera on Microwave Assisted mPE-nHA

The coating of *Aloe vera* on the mPE-nHA was done by the dip-coating method [33]. To start the process, the mPE-nHA samples were dipped in the prepared *Aloe vera* extract. When the samples were completely dipped, the time of dip coating was noted. The *Aloe vera* was dip coated for the period of 12 and 24 h, respectively. After coating, the samples were removed and dried at room temperature for 24 h to remove the moisture on the surface. Most importantly, for each surface and blood compatibility characterization study, samples were freshly prepared as per this protocol. The results for the 12 and 24 h *Aloe-vera*-coated mPE-nHA samples were compared with the pristine mPE-nHA, which was the control. The extract preparation and coating of the *Aloe vera* extract on the mPE-nHA substrate are depicted in Figure 1.

2.8. Characterization of the Samples

2.8.1. Contact Angle Measurement

The hydrophilicity of the *Aloe-vera*-coated mPE-nHA nanocomposite was determined using a Dynamic Contact Angle Analyzer (FTA200—First Ten Angstroms, Portsmouth, VA, USA). A water droplet of 1 µL was used and the photographs were taken in the ultra-fast mode within 30 s. The degree of the angle formed was determined using the computer interfaced software. The contact angles were recorded and analyzed for the pristine, 12 and 24 h *Aloe-vera*-coated mPE-nHA samples (n = 3).

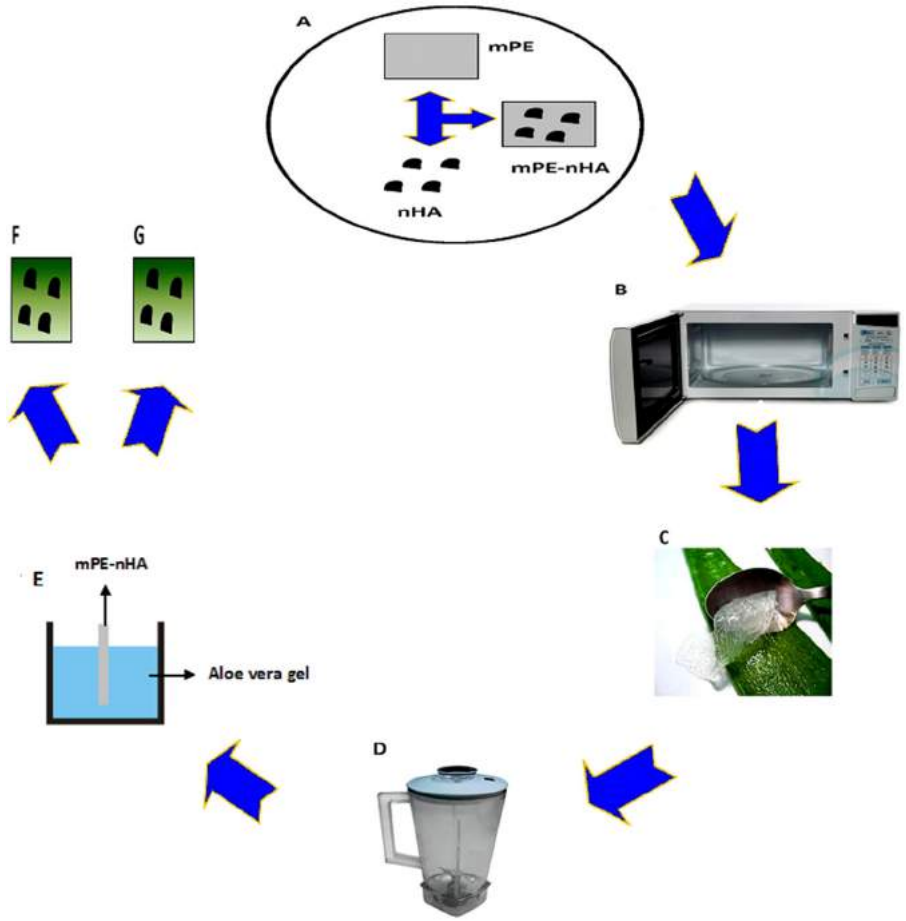

Figure 1. Schematic representation of steps involved in mPE-nHA nanocomposite coating with *Aloe vera*. (**A**) Synthesis of mPE-nHA nanocomposite; (**B**) 60 s microwave treatment; (**C**) Extraction of *Aloe vera*; (**D**) Thorough mixing of the *Aloe vera* gel; (**E**) Dip coating of the *Aloe vera* gel on microwave treated mPE-nHA nanocomposite; (**F**) 12 h *Aloe vera* dip coated mPE-nHA; (**G**) 24 h *Aloe vera* dip-coated mPE-nHA.

2.8.2. Attenuated Total Reflectance Fourier Transfer Infrared Spectroscopy (ATR-FTIR)

The ATR-FTIR equipment NEXUS-870 model spectrophotometer (Thermo Fischer Scientific, Waltham, MA, USA) used has additional features such as an extended beam splitter, two light sources, and middle band MCT detectors with various sampling options. This test was performed to analyze the chemical composition or functional groups present in the *Aloe-vera*-coated nanocomposite and control. Forty scans were obtained per minute and averaged in the resolution of 4 cm^{-1}. Diamond was utilized as the ATR crystal. The FTIR spectra of each sample were recorded separately and the transmittance value corresponding to each wavelength in the region 400–5000 cm^{-1} was imported in an excel sheet using the inbuilt software. Finally, the FTIR outline of each sample analyzed and compared in a single graph using SpekWin version 1.71.6.1 software (Society for Applied Spectroscopy, Berchtesgaden, Germany).

2.8.3. 3D-Hirox Digital Microscope

The 3D-Hirox digital microscope model (KH-8700, Hirox Technologies, Hackensack, NJ, USA) was utilized to study the topography and the *Aloe vera* coating on the samples. 3D-Hirox digital microscopy images are very useful in determining the morphological structure of samples to determine whether the sample has pores or has an even surface. There are two types of images which are obtained from 3D-Hirox digital microscopy either with or without a profilometry line. The surface morphology of 1 cm × 1 cm of mPE-nHA and *Aloe-vera*-coated mPE-nHA samples were studied at an area of 69,277 μm^2

at a magnification of 50×, 100×, 500× and 1000×. The 50× magnification was utilized to study the distribution of the nanohydroxy apaptite in the mPE. The same as in white light confocal profilometry, in-focus and 3D images were obtained using this 3D microscope. Slices of the image were captured at different heights acquired for the surface topography analysis [34]. A maximum of three profiling lines was chosen as the profiling value of each sample. Each point in the *X*, *Y* and *Z* axes of the profiling line was measured and their values were exported to an excel sheet to represent the height of the pits in the sample. Data processing was performed using the in-built 3D profilometry software (3D viewer, Hirox Technologies, Hackensack, NJ, USA). Images were recorded at a standard 1200–1600 pixel resolution.

2.8.4. Scanning Electron Microscope

The surface microstructure of the samples was critically analyzed in detail using SEM (JEOL Ltd., Akishima, Tokyo, Japan). The SEM which was utilized to study the polymeric nanocomposite samples was a JEOL JSM5800 SEM with an OXFORD ISI 300 EDS X-ray microanalysis system (Abingdon, UK). A K550X gold sputter coater, from Quorum Technologies in Lewes, UK was used for sputter coating. The sputter coater had a magnetron target assembly, which enhances the efficiency of the process using low voltages, and provides a fine grain and cool sputtering, without the need to cool the target or the specimen stage which was used. The sputter coating was performed for 4 min. The control and the *Aloe-vera*-coated nanocomposite underwent gold sputtering and was then studied using SEM at a magnification of 1500×.

2.8.5. Atomic Force Microscopy

The surface roughness of the samples in this study was determined with the help of AFM. The AFM model used to analyze the samples was SPA300HV, with a scan rate of 1.502 Hz in the tapping mode. Here, the surface morphology of the pristine and the *Aloe-vera*-coated samples were measured using AFM in contact mode on a 10 × 10 μm^2 area, and the mean average surface roughness (R_a) and the 3D pictographic view were obtained. Each AFM image was analyzed in terms of R_a [35]. The surface roughness was calculated using the SpekWin version 1.71.6.1 software (Society for Applied Spectroscopy, Berchtesgaden, Germany).

2.9. Blood Coagulation Assays

2.9.1. Prothrombin Time (PT)

Prothrombin time is a useful indicator to dictate the prohibition of the extrinsic pathway. Initially, the pristine mPE-nHA, 12 and 24 h *Aloe-vera*-coated mPE-nHA samples of size (1 cm × 1 cm) were placed in separate disposable petri dishes. Then, 100 µL of PPP obtained from citrated whole blood was placed carefully on the samples and incubated in a LABSIL incubator maintained at 37 °C for 3 min. Later, the PPP solution was mixed well with 100 µL of NaCl-thromboplastin Factor III and the time taken for clot formation on each substrate, detected using a steel hook, was measured using a chronometer. The tests were repeated three times independently for each sample [36].

2.9.2. Activated Partial Thromboplastin Time (APTT)

APTT is utilized for studying the propensity of the blood to coagulate via an intrinsic pathway and to determine the effect of a biomaterial on delaying the process. The pristine mPE-nHA, 12 and 24 h *Aloe-vera*-coated mPE-nHA samples of size (1 cm × 1 cm) were placed in separate disposable petri dishes. Then, 100 µL of PPP obtained from citrated whole blood was placed on the samples and incubated at 37 °C for 3 min. Then, the PPP was activated by adding cephaloplastin reagent and again incubated for 5 min at 37 °C. Later, the PPP was activated by the addition of calcium chloride (0.025 $mol \cdot L^{-1}$). The inclusion of $CaCl_2$ triggers the clotting process. The time taken from the addition of $CaCl_2$ to clot formation was noted. Clot formation was indicated by the formation of a thread-like

structure in the blood. The duration taken for the clot formation was recorded with a chronometer as the APTT. The tests were repeated three times independently for each sample [36].

2.9.3. Hemolysis Assay

The pristine and *Aloe-vera*-coated nanocomposites were equilibrated with physiologic saline (0.9% *w*/*v*; 37 °C, 30 min) followed by incubation with 3 mL aliquots of citrated blood diluted with saline (4:5 ratios by volume). This mixture of blood and distilled water was prepared at a ratio of 4:5 by volume to result in comprehensive hemolysis, which was used as the positive control. The physiological saline solution was utilized as the negative control, as it produces no coloration. The samples were subjected to incubation in their respective mixtures (60 min, 37 °C). These mixtures were later centrifuged and their absorbance of the clear supernatant was determined at 542 nm. Finally, the absorbance of the positive control was normalized to 100% and the absorbance of the other samples was ascertained as a percentage of hemolysis whilst comparing it with the positive control [37].

2.10. Statistical Analyses

All the experiments were performed thrice independently. One-way ANOVA was done to determine statistical significance. The results obtained from all experiments are expressed as mean ± SD. In the case of the qualitative experiments, a representative of the three images is shown.

3. Results and Discussion

The mean contact angle of the pristine mPE-nHA was found to be 83° and the mean contact angles of the 12 and 24 h *Aloe vera* dip-coated mPE-nHA samples were 74.5° and 68.15°, respectively, which were significantly lower when compared to the untreated surface as shown in Table 1 and represented in Figure 2. Gentile et al. [38] prepared polyhedral oligomeric silsesquioxane- polycarbonate-based urea urethane (POSS-PCU) composite samples for bone tissue engineering and performed plasma treatment. It was observed that the initial pure POSS-PCU composite samples were hydrophobic with a contact angle of 90 ± 4° and after 10 min plasma modified composite films exhibited a hydrophilic nature with a contact angle of 53 ± 5°. Our contact angle results were found to be in a similar trend as they observed what predicts the suitability of the developed composite for bone tissue engineering.

FTIR was performed for the determination of the chemical composition of untreated and treated samples, as shown in Figure 3. The peaks were observed at 714, 1014, 1232, 1369, 1469, 1583, 1731, 2845, 2912, and 3363 cm^{-1}. The patterns of peaks with differing intensities were noted for both control and coated samples. The 3363 cm^{-1} represents the O–H stretching of the alcohol group. The drastic increase in the intensity of this peak for the 24 h *Aloe vera* dip-coated mPE-nHA dictates the improved hydrophilicity of the coated samples compared to the control. The twin bands at 2845 and 2912 cm^{-1} ascertain the presence of C–H stretch for the alkanes group. The absorption peak at 1731 cm^{-1} was for the C=O stretch of esters; the peak observed at 1469 cm^{-1} dictates the presence of alkyl groups (C–H bending), and the existence of C–H bending of the alkane group is inferred from the peak produced at 1369 cm^{-1}. The peak at 1583 cm^{-1} represents the C=C stretching in the cyclic alkene group. The absorption band in the region of 1232 cm^{-1} denotes the C–O stretch of carboxylic acids (controls), and the crest at 1014 cm^{-1} represents the C–O stretch in secondary alcohol. Finally, the peak at 714 cm^{-1} represents the C–H bend of the aromatic and alkyne group, respectively. In spite of there being no major change in the functional groups, the *Aloe vera* dip-coated mPE-nHA nanocomposite samples demonstrated characteristic absorption spectrum of *Aloe vera* at 1731 and 1232 cm^{-1}, elucidating the presence of O-acetyl esters; the peaks formed at 1469 cm^{-1} and 714 cm^{-1} unravelled the essence of the aromatic vibrations of the components present in *Aloe vera* gel [39,40]. In the interim, the *Aloe vera* dip-coated samples were also found to have peak shifts at far regions of the IR spectra ("Zone A"), which shown in Figure 3b. The peaks shifts were represented in Table 2. These shifts were supposed to appear owing to the presence of the minerals available in *Aloe vera*

gel. This result is in accordance with the peaks formed between 400–500 cm^{-1} and 500–600 cm^{-1}, demonstrating Si–O bending and C–H stretch as in some previous studies [41].

Table 1. Contact angle measurement of the mPE before and after HNO_3 treatment.

Sample Number	Sample	Average Contact Angle in Degrees *
1	Pristine mPE-nHA	83
2	mPE-nHA coated with *Aloe vera* (12 h)	74.5
3	mPE-Nha coated with *Aloe vera* (24 h)	68.15

* Differences were significant compared with pristine mPE-nHA ($p < 0.05$).

Table 2. Peak shifts observed in Zone A of the recorded FTIR.

Pristine mPE-nHA	12 h *Aloe-Vera*-Treated mPE-nHA	24 h *Aloe-Vera*-Treated mPE-nHA
406	416	424
428	431	436
444	451	464
457	466	470
471	480	474
476	486	480
486	497	486
503	515	509
528	535	532

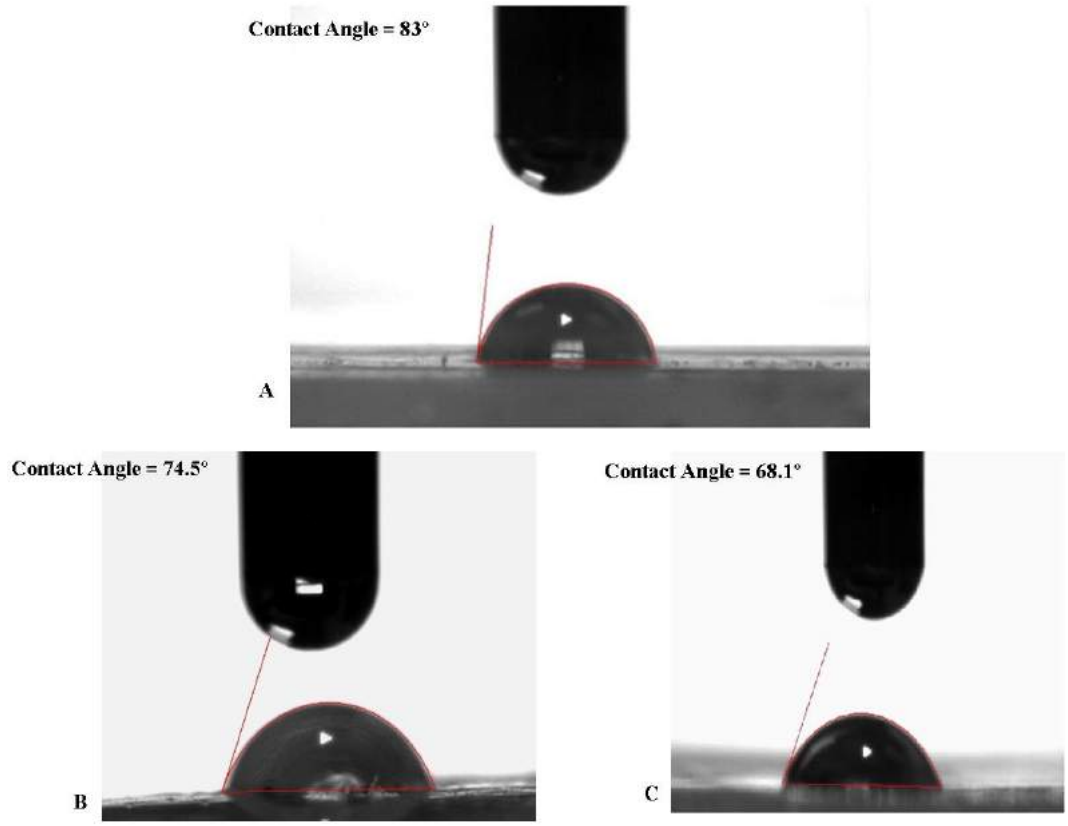

Figure 2. A representative contact angle image showing the spreading of a water droplet in pristine mPE-nHA, and 12 and 24 h *Aloe vera* dip-coated mPE-nHA ($n = 3$), respectively.

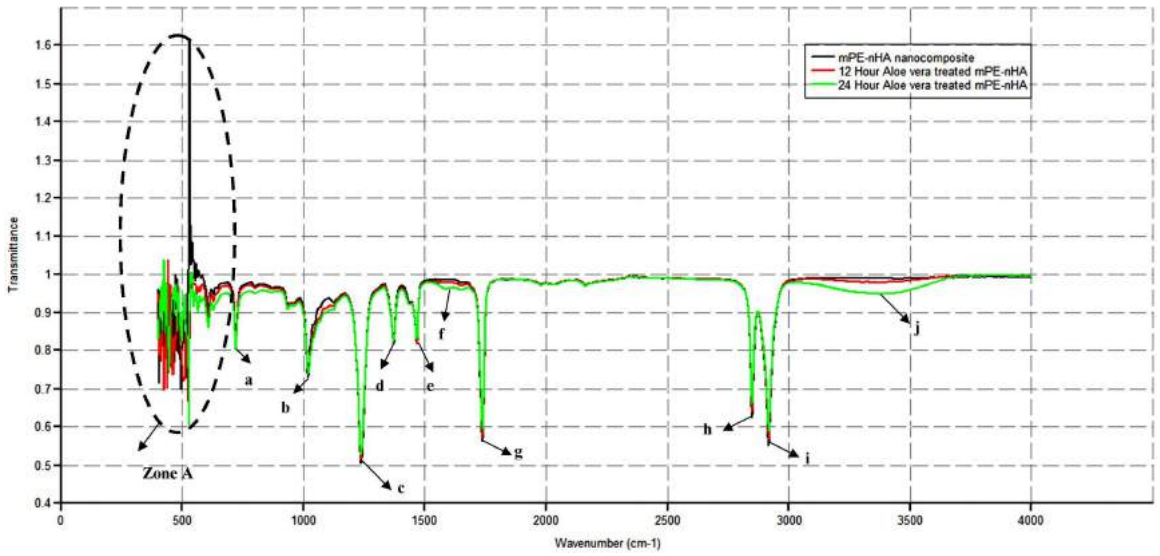

Figure 3. A representative FTIR spectra of pristine mPE-nHA, 12 and 24 h *Aloe vera* dip-coated mPE-nHA nanocomposites. (**a**) 714 cm^{-1}, (**b**) 1014 cm^{-1}, (**c**) 1232 cm^{-1}, (**d**) 1369 cm^{-1}, (**e**) 1469 cm^{-1}, (**f**) 1583 cm^{-1}, (**g**) 1731 cm^{-1}, (**h**) 2845 cm^{-1}, (**i**) 2912 cm^{-1}, (**j**) 3363 cm^{-1}.

Figure 4 represents the 100× and 500× 3D Hirox digital microscopy images of mPE-nHA and *Aloe vera* dip-coated mPE-nHA. A tangible coating of *Aloe vera* was observed after the 12 and 24 h exposure to *Aloe vera* extracts. Figure 5A shows the distribution of hydroxyapatite nanorods in the mPE sample. It was found that the area ratio of nHA was 7.6% and the distribution of the nHA nanorod analysis in mPE-nHA depicts that there are 184 nHA nanorods present in a 2,144,112 μm^2 area. The thickness of the *Aloe vera* coating measured was found to be 94.8 µm for the 24 h *Aloe vera* dip-coated mPE-nHA, as represented in Figure 5B. Figure 5C–E further shows that the 1000× images of 3D hirox further dictate the presence of the fibrous *Aloe vera* structure, which is present in the 12 h and 24 h *Aloe vera* dip-coated mPE-nHA, and absent in the pristine mPE-nHA. Figure 6 ascertains the profiling lines of the mPE-nHA surface at 1000× magnification, where the thickness of the *Aloe vera* coating was found to be the highest for the 24 h *Aloe vera* dip-coated mPE-nHA. Al-Hijazi et al. [42] studied the biological effect of *Aloe vera* in bone healing and also investigated the expression of bone morphogenetic protein 7 (BMP7) in *Aloe vera* treated bone tissue. It was observed that the *Aloe vera* treated group exhibited increased proliferation of osteogenic cells and enhanced the expression of BMP7 compared to the untreated group. Hence in our prepared composites containing significant amounts of *Aloe vera* content might favor the enhanced proliferation of osteogenic cells for new bone tissue growth.

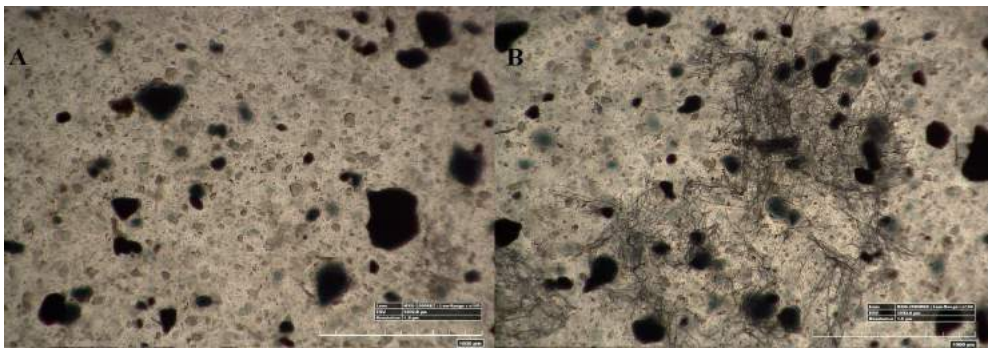

Figure 4. *Cont.*

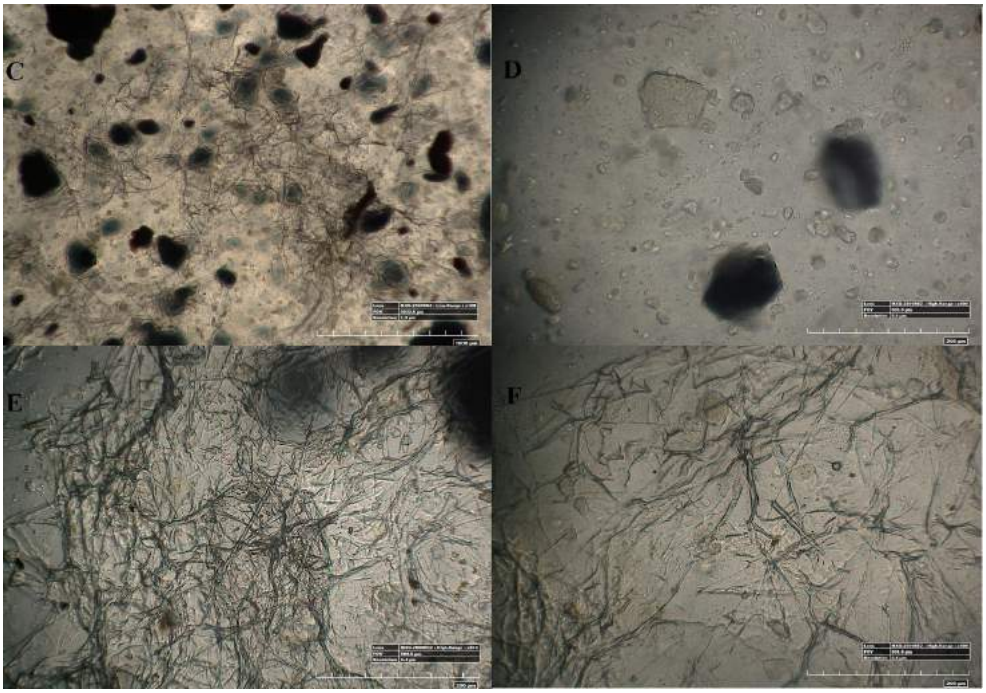

Figure 4. 100× and 500× image using 3D Hirox digital microscopy. (**A**–**C**) are the 100× image of pristine mPE-nHA, 12 h *Aloe vera* dip-coated mPE-nHA and 24 h *Aloe vera* dip-coated mPE-nHA nanocomposite, respectively; (**D**–**F**) are the 500× images of untreated mPE-nHA, 12 h *Aloe vera* dip-coated mPE-nHA and 24 h *Aloe vera* dip-coated mPE-nHA nanocomposite, respectively.

Figure 7 shows the representative SEM micrographs of pristine and *Aloe vera* dip-coated mPE-nHA. The bright spots represent the pits that may have formed in the pristine mPE-nHA due to the surface-modification effect of the microwave. These pits were later concealed by *Aloe vera* gel in the dip-coated samples. It is evident that the *Aloe vera* coating is greater even in the case of the 24 h *Aloe vera* dip-coated samples compared to the 12 h *Aloe vera* sample, which illustrates that the coating is time-dependent. Further, the bright spots formed in the mPE-nHA depict the improved surface roughness by the formation of pits. For bone tissue engineering, the material with enhanced surface roughness will favor the adhesion and proliferation of osteoblasts for bone tissue growth [43]. The prepared mPE-nHA nanocomposites render rougher surfaces which might enhance the adhesion and proliferation of osteoblasts for new bone tissue growth.

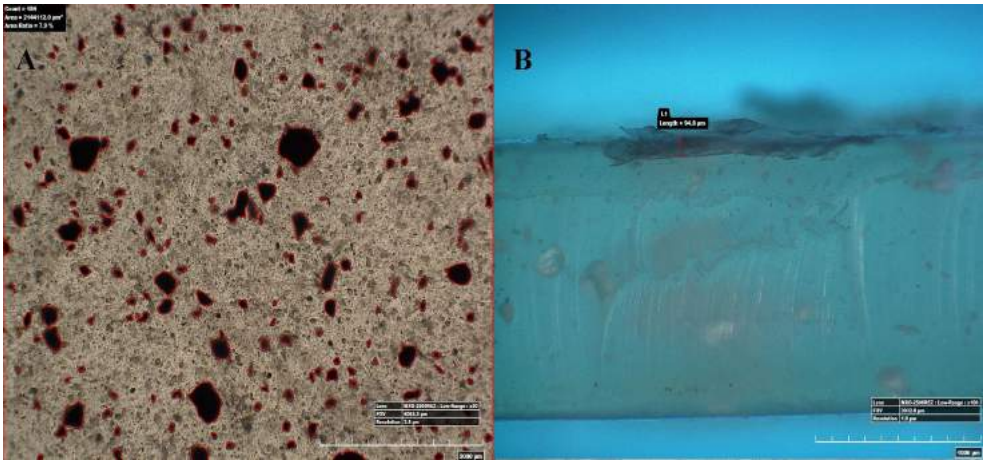

Figure 5. *Cont.*

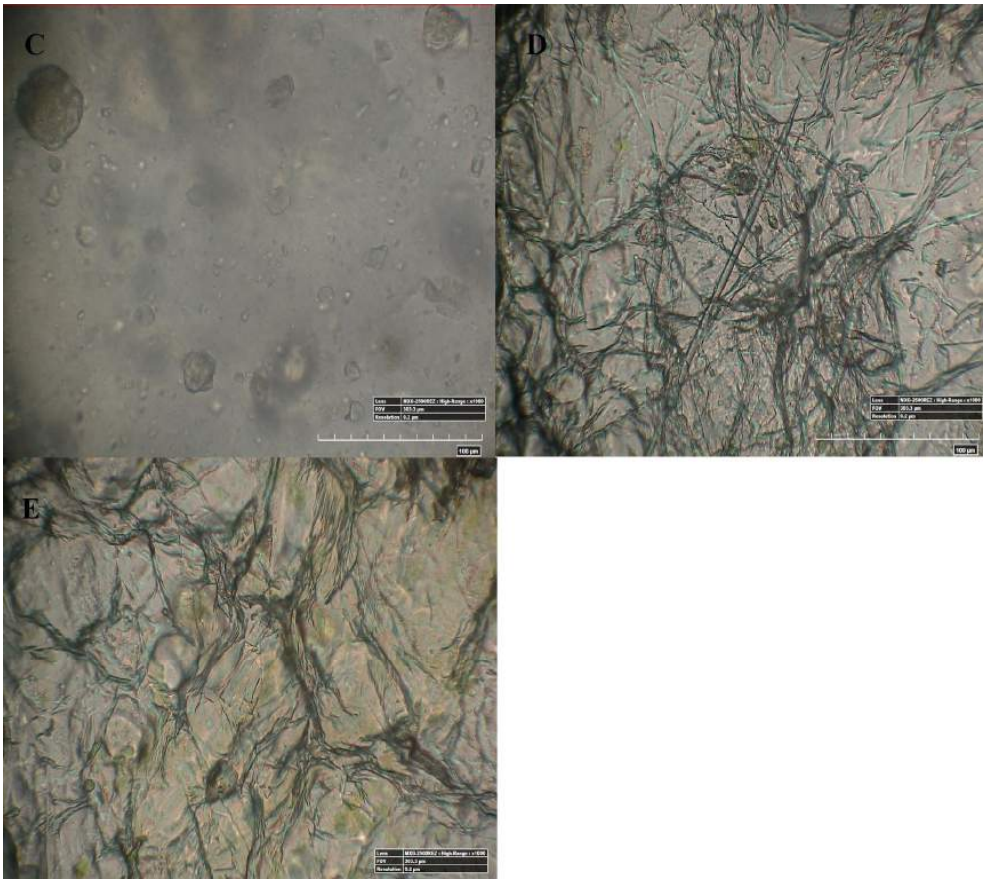

Figure 5. 50×, 100× and 1000× image using 3D Hirox digital microscopy. (**A**) nHA nanorod distribution in pristine mPE-nHA at 50×; (**B**) Thickness of *Aloe vera* coating in 24 h *Aloe vera* dip-coated mPE-nHA at 100×; (**C**–**E**) are 1000× images of untreated mPE-nHA, and 12 and 24 h *Aloe vera* dip-coated mPE-nHA, respectively.

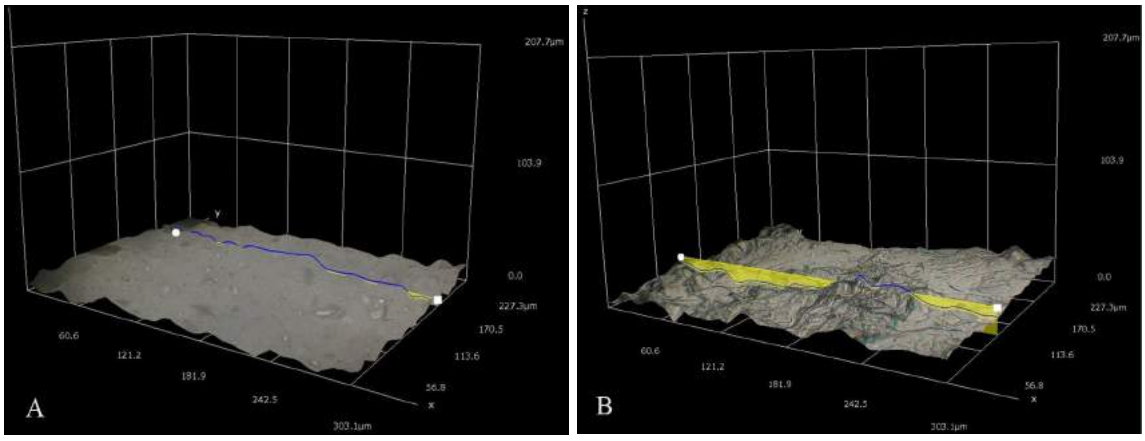

Figure 6. *Cont.*

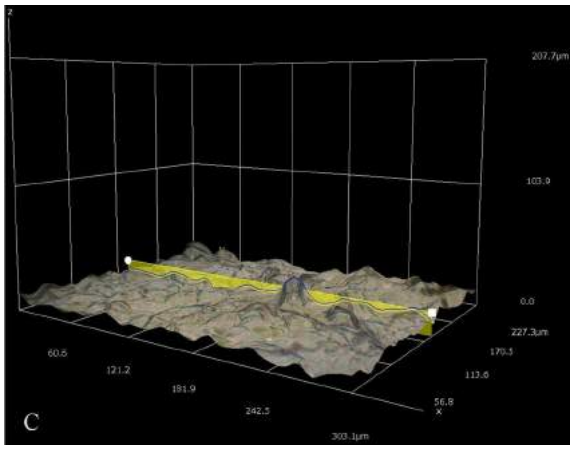

Figure 6. Different three-dimensional representations using 3D Hirox digital microscopy. (**A**) Profiling of pristine mPE-nHA at 1000×; (**B**) Profiling of 12 h *Aloe vera* dip-coated mPE-nHA at 1000×; (**C**) Profiling of 24 h *Aloe vera* dip-coated mPE-nHA at 1000×.

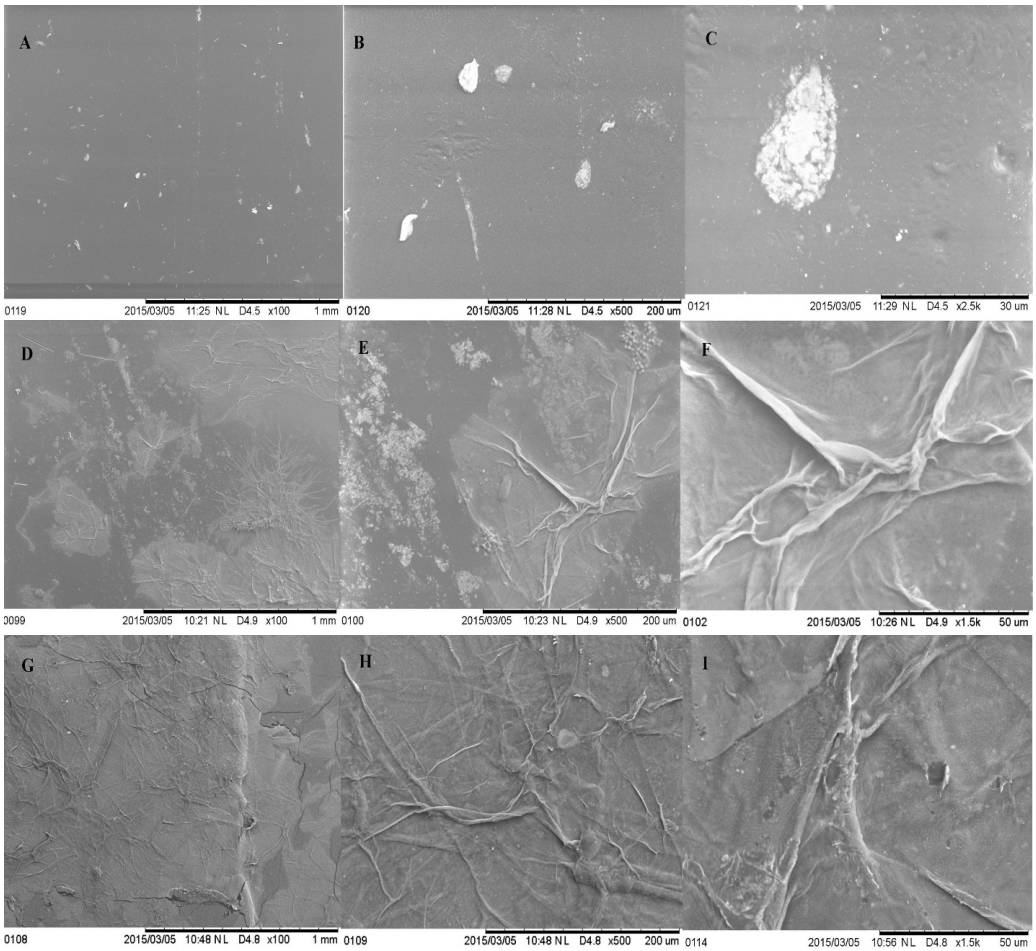

Figure 7. Representative SEM micrographs of pristine and *Aloe vera* dip-coated mPE-nHA. (**A**) Pristine mPE-nHA at 100×; (**B**) mPE-nHA at 500×; (**C**) mPE-nHA at 2500×; (**D**) 12 h *Aloe vera* dip-coated mPE-nHA at 100×; (**E**) 12 h *Aloe vera* dip-coated mPE-nHA at 500×; (**F**) 12 h *Aloe vera* dip-coated mPE-nHA at 1500×; (**G**) 24 h *Aloe vera* dip-coated mPE-nHA at 100×; (**H**) 24 h *Aloe vera* dip-coated mPE-nHA at 500×; (**I**) 24 h *Aloe vera* dip-coated mPE-nHA at 1500×.

The AFM images are given in Figure 8. It was found that the mean value of the average surface roughness R_a of the pristine mPE-nHA film and 24 h *Aloe vera* dip-coated mPE-nHA film surfaces were 1.17 and 7.52 nm, respectively. The nanotopographic analysis of the samples was demonstrated utilizing AFM (NanoWizard®, JPK Instruments, Berlin, Germany). Figure 8A represents the 3D surface topography of the pristine mPE-nHA nanocomposite. It was observed that the surface of the sample possess smaller number of hill and valley structures in the untreated mPE-nHA nanocomposite sample. In contrast, Figure 8B, which shows 60 s microwave treated and 24 h *Aloe vera* dip-coated mPE-nHA, indicates more nano-roughness. Jose et al. prepared bioactive polysulfone nanocomposites blended with hydroxyapatite for bone tissue engineering. The surface roughness (R_a) of pure polysulfone was found to be 2.22, and the 1, 2 and 5 wt % loading of hydroxyapatite fillers were found to be 3.85, 4.97 and 7.80, respectively; our results show similar roughness levels [44]. It was reported that bone implant with enhanced roughness has a significant influence on the adhesion and proliferation of osteoblasts [40], hence our *Aloe vera* dip-coated mPE-nHA with enhanced roughness might be suitable for the bone tissue engineering.

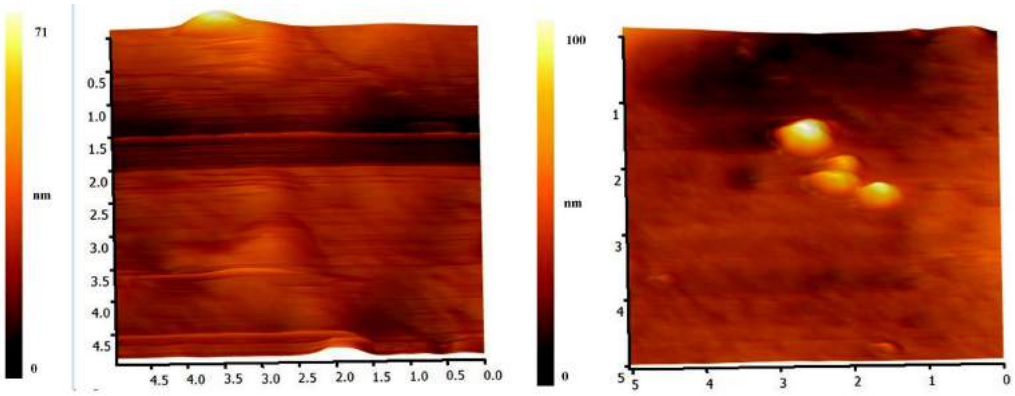

(**A**) (**B**)

Figure 8. Representative AFM images of pristine and *Aloe vera* dip-coated mPE-nHA. (**A**) Pristine mPE-nHA; (**B**) 24 h *Aloe vera* dip-coated mPE-nHA.

The results of the PT and APTT are summarized in Figure 9. Both the PT and APTT demonstrated an increase in their value for 12 and 24 h *Aloe vera* dip-coated mPE-nHA compared to the pristine mPE-nHA. The mean PT of the mPE-nHA nanocomposite control and 12 h and 24 h *Aloe vera* dip-coated mPE-nHA was 48, 49 and 51 s, respectively. The PT was prolonged by 1.06 percent after dip coating with *Aloe vera*, which is in the similar trend found in a study where the PT time was found to be delayed in thermoplastic polyurethane (TPU) by 1.9 times following dextran coating. On the other hand, the mean APTT was found to be 179, 210 and 220 s, respectively. Statistical analysis of the untreated sample with the treated ones using one-way ANOVA showed significant differences ($p < 0.05$) between them for APTT. The hemolysis assay was performed for studying the effect of *Aloe vera* dip-coating on the red blood cells (RBC). Mean absorbance seemed to reduce in the case of *Aloe vera* dip-coated samples compared with pristine mPE-nHA, indicating lesser damage incurred by the interaction between the samples and the RBC, as shown in Figure 10. The mean absorbance was found to be 0.6533, 0.0143, 0.0046, and 0.0016 for the positive control, mPE-nHA nanocomposite, 12 h *Aloe vera* dip-coated mPE-nHA and 24 h *Aloe vera* dip-coated mPE-nHA, respectively. The computed hemolytic percentages were found to be 8.158%, 2.188%, 0.704%, and 0.2449% for the above-mentioned samples, respectively. Statistical analysis of the percentage of hemolysis of the mPE-nHA nanocomposite and the *Aloe vera* dip-coated mPE-nHA samples using one-way ANOVA dictated a statistically significant ($p < 0.05$) decrease in hemolytic percentage for the *Aloe vera* dip-coated mPE-nHA samples compared to the control pristine mPE-nHA. From the results obtained, it is obvious that the 24 h *Aloe vera* dip-coated mPE-nHA is the least hemolytic compared to the other samples. According to ASTMF756-00(2000) standard [45], mPE-nHA nanocomposite, 12 h *Aloe vera* dip-coated mPE-nHA and 24 h *Aloe vera*

dip-coated mPE-nHA is inferred to be a non-hemolytic material, since the percentage of damage falls below two percent. Selvakumar et al. [27] prepared a nanocomposite based on polyurethane incorporated with polypropylene glycol (PPG)-warped hydroxyapatite for bone tissue engineering. It was observed that the hydroxyapatite-loaded polyurethane nanocomposites exhibited enhanced blood compatibility and also observed enhanced osteoblast MG63 cell proliferation compared to pristine polyurethane (PU). Hence, our developed membrane showing enhanced blood compatibility might favor osteoblast cell proliferation for new bone tissue growth.

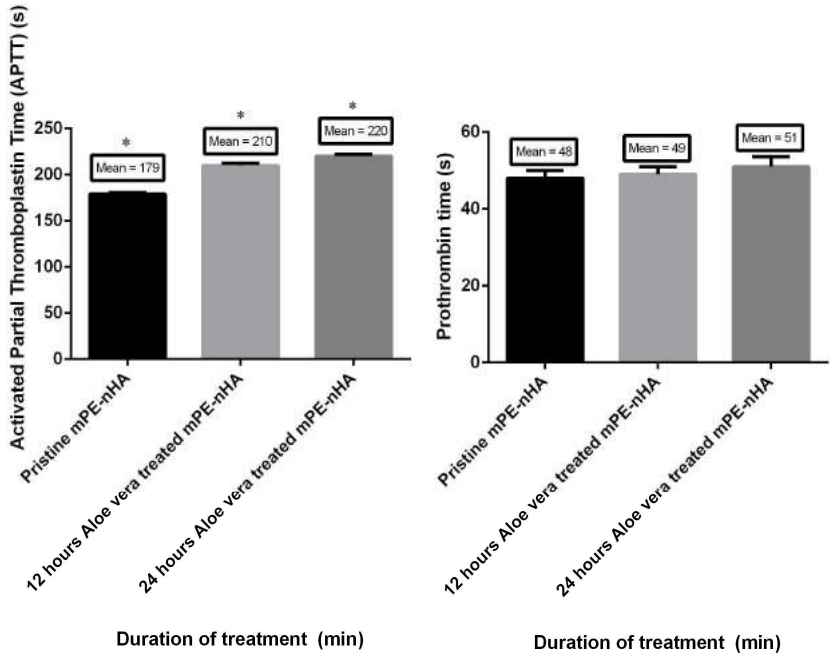

Figure 9. Comparison of prothrombin time (PT), activated partial thromboplastin time (APPT) and absorbance of pristine mPE-nHA, 12 h and 24 h *Aloe vera* dip-coated mPE-nHA (n = 3). Values shown are mean ± SD and * indicates that differences in the mean are significant ($p < 0.05$) with respect to the mPE control.

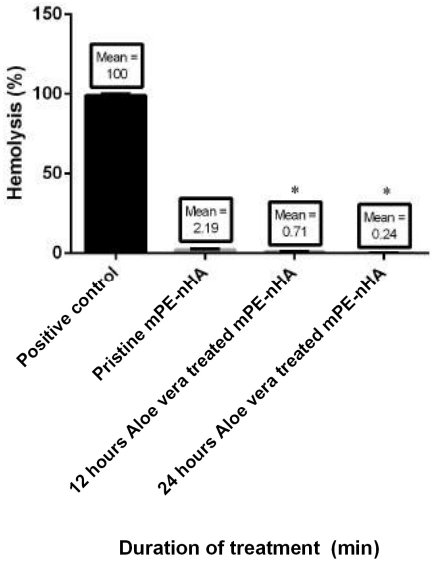

Figure 10. Comparison of the hemolysis percentage of the positive control, pristine mPE-nHA, 12 h and 24 h *Aloe vera* dip-coated mPE-nHA (n = 3). Values shown are mean ± SD and * indicates that differences in the mean are significant ($p < 0.05$) with respect to the mPE control.

4. Conclusions

In this study, the mPE was incorporated with nano-rods of hydroxyapaptite and then coated with *Aloe vera* with the help of a microwave. The samples were subjected to physical characterization tests such as contact angle, FTIR, SEM, AFM and 3D Hirox microscopy scanning. The results show that the hydrophilicity of the nano-hydroxyapaptite improves with dip coating with *Aloe vera*. The *Aloe vera* juice makes the surface topology of the mPE-nHA more hydrophilic, thereby improving its wettability. Surface roughness improvement was ascertained by the AFM result. The presence of *Aloe vera* dip coating on mPE-nHA was confirmed by the SEM and 3D Hirox microscopy results. The PT was delayed by 1.06% for the 24 h *Aloe vera* dip-coated mPE-nHA compared to the pristine mPE-nHA. Likewise, the *Aloe vera* dip-coated mPE-nHA nanocomposite prolonged the APTT by 41 s against the pristine mPE-nHA. The hemolysis percentage was found to be the least for the 24 h *Aloe vera* dip-coated mPE-nHA nanocomposite, which was only 0.2449%. Hence, the 24 h *Aloe vera* dip-coated mPE-nHA can be plausibly exploited for bone tissue engineering applications.

Acknowledgments: This work was supported by the Ministry of Higher Education Malaysia with the Grant no.Q.J130000.2545.17H00 and FRGS Grant no.R.J130000.7809.4F444.

Author Contributions: Hairong Wang and Xueliang Zhang performed the experiments and analyzed the data. Mohan Prasath Mani assisted in doing the experiments, analyzed the data, wrote the paper, and prepared figures and/or tables. Saravana Kumar Jaganathan conceived and designed the experiments, performed the experiments, analyzed the data, contributed reagents/materials/analysis tools, prepared figures and/or tables and reviewed drafts of the paper. Yi Huang and Chengzheng Wang contributed reagents/materials/analysis tools and reviewed drafts of the paper.

Conflicts of Interest: The authors declare no conflict of interest.

References

1. O'brien, F.J. Biomaterials & scaffolds for tissue engineering. *Mater. Today* **2011**, *14*, 88–95.
2. Zohora, F.T.; Azim, A.Y.M.A. Biomaterials as a porous scaffold for tissue engineering applications: A review. *Eur. Sci.* **2014**, *10*, 186–209.
3. Kar, K.K.; Rana, S.; Pandey, J. *Handbook of Polymer Nanocomposites Processing, Performance and Application*; Springer: Berlin/Heidelberg, Germany, 2015.
4. De Santis, R.; Gloria, A.; Russo, T.; D'Amora, U.; Zeppetelli, S.; Dionigi, C.; Sytcheva, A.; Herrmannsdorfer, T.; Dediu, V.; Ambrosio, L. A basic approach toward the development of nanocomposite magnetic scaffolds for advanced bone tissue engineering. *J. Appl. Polym. Sci.* **2011**, *122*, 3599–3605. [CrossRef]
5. Gloria, A.; Russo, T.; D'Amora, U.; Zeppetelli, S.; D'Alessandro, T.; Sandri, M.; Bañobre-López, M.; Piñeiro-Redondo, Y.; Uhlarz, M.; Tampieri, A.; et al. Magnetic poly(epsilon-caprolactone)/iron-doped hydroxyapatite nanocomposite substrates for advanced bone tissue engineering. *J. R. Soc. Interface* **2013**, *10*, 20120833. [CrossRef] [PubMed]
6. Dorozhkin, S.V. *Calcium Orthophosphates: Applications in Nature, Biology, and Medicine*; CRC Press: Boca Raton, FL, USA, 2012; p. 854.
7. Eliaz, N.; Metoki, N. Calcium phosphate bioceramics: A review of their history, structure, properties, coating technologies and biomedical applications. *Materials* **2017**, *10*, 334. [CrossRef] [PubMed]
8. Huber, F.X.; McArthur, N.; Hillmeier, J.; Kock, H.J.; Baier, M.; Diwo, M.; Berger, I.; Meeder, P.J. Void filling of tibia compression fracture zones using a novel resorbable nanocrystalline hydroxyapatite paste in combination with a hydroxyapatite ceramic core: First clinical results. *Arch. Orthop. Trauma Surg.* **2006**, *126*, 533–540. [CrossRef] [PubMed]
9. Banobre-Lopez, M.; Pineiro-Redondo, Y.; De Santis, R.; Gloria, A.; Ambrosio, L.; Tampieri, A.; Dediu, V.; Rivas, J. Poly(caprolactone) based magnetic scaffolds for bone tissue engineering. *J. Appl. Phys.* **2011**, *109*, 07B313. [CrossRef]
10. Fu, S.; Wang, X.; Guo, G.; Shi, S.; Liang, H.; Luo, F.; Wei, Y.; Qian, Z. Preparation and characterization of nano-hydroxyapatite/poly(ε-caprolactone)-poly(ethylene glycol)-poly(ε-caprolactone) composite fibers for tissue engineering. *J. Phys. Chem. C* **2010**, *114*, 18372–18378. [CrossRef]

11. Laschke, M.W.; Strohe, A.; Menger, M.D.; Alini, M.; Eglin, D. In vitro and in vivo evaluation of a novel nanosize hydroxyapatite particles/poly(ester-urethane) composite scaffold for bone tissue engineering. *Acta Biomater.* **2010**, *6*, 2020–2027. [CrossRef] [PubMed]
12. Ma, R.; Weng, L.; Bao, X.; Ni, Z.; Song, S.; Cai, W. Characterization of in situ synthesized hydroxyapatite/polyetheretherketone composite materials. *Mater. Lett.* **2012**, *71*, 117–119. [CrossRef]
13. Hamman, H.H. Composition and applications of *Aloe vera* leaf gel. *Molecules* **2008**, *13*, 1599–1616. [CrossRef] [PubMed]
14. Surjushe, A.; Vasani, R.; Saple, D.G. *Aloe vera*: A short review. *Ind. J. Dermatol.* **2008**, *53*, 163–166. [CrossRef] [PubMed]
15. Herzberg, F.; Gruenwald, J. *Aloe Vera: An International Success Story*; Nutraceutical World: Ramsey, NJ, USA, 2003.
16. Davis, R.H.; Donato, J.J.; Hartman, G.M.; Haas, R.C. Anti-inflammatory and wound healing activity of a growth substance in *Aloe vera*. *J. Am. Podiatr. Med. Assoc.* **1994**, *84*, 77–81. [CrossRef] [PubMed]
17. Guruvenket, S.; Rao, G.M.; Komath, M.; Raichur, A.M. Plasma surface modification of polystyrene and polyethylene. *Appl. Surf. Sci.* **2004**, *236*, 278–284. [CrossRef]
18. Hui, A.Y.N.; Wang, G.; Lin, B.; Chan, W.T. Microwave plasma treatment of polymer surface for irreversible sealing of microfluidic devices. *Lab Chip* **2005**, *5*, 1173–1177. [CrossRef] [PubMed]
19. Ku, H.S.; Siores, E.; Ball, J.A.R. Review—Microwave processing of materials: Part I. *HKIE Trans.* **2001**, *8*, 31–37.
20. Kavya, K.C.; Dixit, R.; Jayakumar, R.; Nair, S.V.; Chennazhi, K.P. Synthesis and characterization of chitosan/chondroitin sulfate/nano-SiO_2 composite scaffold for bone tissue engineering. *J. Biomed. Nanotechnol.* **2012**, *8*, 149–160. [CrossRef] [PubMed]
21. Zhou, S.; Zheng, X.; Yu, X.; Wang, J.; Weng, J.; Li, X.; Feng, B.; Yin, M. Hydrogen bonding interaction of poly(d,l-lactide)/hydroxyapatite nanocomposites. *Chem. Mater.* **2007**, *19*, 247–253. [CrossRef]
22. Gong, X.H.; Tang, C.Y.; Hu, H.C.; Zhou, X.P.; Xie, X.L. Improved mechanical properties of HIPS/hydroxyapatite composites by surface modification of hydroxyapatite via in-situ polymerization of styrene. *J. Mater. Sci. Mater. Med.* **2004**, *15*, 1141–1146. [CrossRef] [PubMed]
23. Lee, H.J.; Choi, K.W.; Kim, K.J.; Lee, S.C. Modification of hydroxyapatite nanosurfaces for enhanced colloidal stability and improved interfacial adhesion in nanocomposites. *Chem. Mater.* **2006**, *18*, 5111–5118. [CrossRef]
24. Bose, S.; Saha, S.K. Synthesis and characterization of hydroxyapatite nanopowders by emulsion technique. *Chem. Mater.* **2003**, *15*, 4464–4469. [CrossRef]
25. Yuan, J.; Wu, Y.; Zheng, Q.X.; Xie, X.L. Synthesis and characterization of nano hydroxylapatite by reaction precipitation in impinging streams. *Adv. Mater. Res.* **2011**, *160*, 1301–1308. [CrossRef]
26. Vidhya, G.; Kumar, G.S.; Kattimani, V.S.; Thamizhavel, A.; Girija, E.K. Microwave irradiation synthesis of 3D flower-like hydroxyapatite. *Int. J. Sci. Eng. Res.* **2015**, *6*, 18–19.
27. Selvakumar, M.; Jaganathan, S.K.; Nando, G.B.; Chattopadhyay, S. Synthesis and characterization of novel polycarbonate based polyurethane/polymer wrapped hydroxyapatite nanocomposites: Mechanical properties, osteoconductivity and biocompatibility. *J. Biomed. Nanotechnol.* **2015**, *11*, 291–305. [CrossRef] [PubMed]
28. Irzh, A.; Gedanken, A. A microwave-assisted process for coating polymer and glass surfaces with semiconducting ZnO submicron particles. *J. Appl. Polym. Sci.* **2009**, *113*, 1773–1780. [CrossRef]
29. Irzh, A.; Perkas, N.; Gedanken, A. Microwave-assisted coating of PMMA beads by silver nanoparticles. *Langmuir* **2007**, *23*, 9891–9897. [CrossRef] [PubMed]
30. Su, H.C.; Chen, C.H.; Chen, Y.C.; Yao, D.J.; Chen, H.; Chang, Y.C.; Yew, T.R. Improving the adhesion of carbon nanotubes to a substrate using microwave treatment. *Carbon* **2010**, *48*, 805–812. [CrossRef]
31. Tuval, T.; Gedanken, A. A microwave-assisted polyol method for the deposition of silver nanoparticles on silica spheres. *Nanotechnology* **2007**, *18*, 255601. [CrossRef]
32. Mohandas, H.; Sivakumar, G.; Kasi, P.; Jaganathan, S.K.; Supriyanto, E. Microwave-assisted surface modification of metallocene polyethylene for improving blood compatibility. *BioMed Res. Int.* **2013**, *2013*, 253473. [CrossRef] [PubMed]
33. Xue, L.; Gao, X.; Zhao, K.; Liu, J.; Yu, X.; Han, Y. The formation of different structures of poly(3-hexylthiophene) film on a patterned substrate by dip coating from aged solution. *Nanotechnology* **2010**, *21*, 145303. [CrossRef] [PubMed]

34. Pereira, C.; Busani, T.; Branco, L.C.; Joosten, I.; Sandu, I.C. Nondestructive characterization and enzyme cleaning of painted surfaces: Assessment from the macro to nano level. *Microsc. Microanal.* **2013**, *19*, 1632–1644. [CrossRef] [PubMed]
35. Pelagade, S.M.; Rane, R.S.; Mukherjee, S.; Deshpande, U.P.; Ganesan, V.; Shripathi, T. Investigation of surface free energy for PTFE polymer by bipolar argon plasma treatment. *J. Surf. Eng. Mater. Adv. Technol.* **2012**, *2*, 132–136. [CrossRef]
36. Amarnath, L.P.; Srinivas, A.; Ramamurthi, A. In vitro hemocompatibility testing of UV-modified hyaluronan hydrogels. *Biomaterials* **2006**, *27*, 1416–1424. [CrossRef] [PubMed]
37. Jaganathan, S.K.; Mohandas, H.; Sivakumar, G.; Kasi, P.; Sudheer, T.; Avineri, V.S.; Murugesan, S.; Supriyanto, E. Enhanced blood compatibility of metallocene polyethylene subjected to hydrochloric acid treatment for cardiovascular implants. *BioMed Res. Int.* **2014**, *2014*, 963149. [CrossRef] [PubMed]
38. Gentile, P.; Ghione, C.; Tonda-Turo, C.; Kalaskar, D.M. Peptide functionalisation of nanocomposite polymer for bone tissue engineering using plasma surface polymerisation. *RSC Adv.* **2015**, *5*, 80039–80047. [CrossRef]
39. Agnes Mary, S.; Giri Dev, V.R. Electrospun herbal nanofibrous wound dressings for skin tissue engineering. *J. Text. Inst.* **2015**, *106*, 886–895. [CrossRef]
40. Suganya, S.; Venugopal, J.; Ramakrishna, S.; Lakshmi, B.S.; Dev, V.R. Naturally derived biofunctional nanofibrous scaffold for skin tissue regeneration. *Int. J. Biol. Macromol.* **2014**, *68*, 135–143. [CrossRef] [PubMed]
41. Müller, C.M.; Pejcic, B.; Esteban, L.; Piane, C.D.; Raven, M.; Mizaikoff, B. Infrared attenuated total reflectance spectroscopy: An innovative strategy for analyzing mineral components in energy relevant systems. *Sci. Rep.* **2014**, *4*, 6764. [CrossRef] [PubMed]
42. Al-Hijazi, A.Y.; Al-Mahammadawy, A.K.; Issa, E. Expression of BMP7 in bone tissue treated with *Aloe vera*. *Int. Res. J. Natl. Sci.* **2015**, *3*, 39–48.
43. Huang, H.H.; Ho, C.T.; Lee, T.H.; Lee, T.L.; Liao, K.K.; Chen, F.L. Effect of surface roughness of ground titanium on initial cell adhesion. *Biomol. Eng.* **2004**, *21*, 93–97. [CrossRef] [PubMed]
44. Jose, A.J.; Alagar, M. Development of bioactive polysulfone nanocomposites for bone tissue replacement. In Proceedings of the 18th International Conference on Composite Materials (ICCM-18), Jeju Island, Korea, 21–26 August 2011.
45. *ASTM F756-00 Standard Practice for Assessment of Hemolytic Properties of Materials*; ASTM International: West Conshohocken, PA, USA, 2000.